

See discussions, stats, and author profiles for this publication at: <https://www.researchgate.net/publication/220781355>

# Fingerprint Image Enhancement Using STFT Analysis

Conference Paper *in* Lecture Notes in Computer Science · August 2005

DOI: 10.1007/11552499\_3 · Source: DBLP

CITATIONS

129

READS

537

3 authors, including:



Venu Govindaraju

University at Buffalo, The State University of New York

400 PUBLICATIONS 7,958 CITATIONS

SEE PROFILE



Alexander N. Cartwright

University at Buffalo, The State University of New York

248 PUBLICATIONS 3,628 CITATIONS

SEE PROFILE

Some of the authors of this publication are also working on these related projects:



Thermal Mechanical Behavior of BGA Solder Joints [View project](#)

# Fingerprint Image Enhancement Using STFT Analysis

Sharat Chikkerur \*, Venu Govindaraju, and Alexander N. Cartwright

Center for Unified Biometrics and Sensors, University at Buffalo, NY, USA

**Abstract.** Contrary to popular belief, despite decades of research in fingerprints, reliable fingerprint recognition is still an open problem. Extracting features out of poor quality prints is the most challenging problem faced in this area. This paper introduces a new approach for fingerprint enhancement based on Short Time Fourier Transform(STFT) Analysis. STFT is a well known technique in signal processing to analyze non-stationary signals. Here we extend its application to 2D fingerprint images. The algorithm simultaneously estimates all the intrinsic properties of the fingerprints such as the foreground region mask, local ridge orientation and local frequency orientation. We have evaluated the algorithm over a set of 800 images from FVC2002 DB3 database and obtained a 17% relative improvement in the recognition rate.

## 1 Introduction

The performance of a fingerprint feature extraction and matching algorithm depends critically upon the quality of the input fingerprint image. While the 'quality' of a fingerprint image cannot be objectively measured, it roughly corresponds to the clarity of the ridge structure in the fingerprint image. Where as a 'good' quality fingerprint image has high contrast and well defined ridges and valleys, a 'poor' quality fingerprint is marked by low contrast and ill-defined boundaries between the ridges. There are several reasons that may degrade the quality of a fingerprint image.

1. Presence of creases, bruises or wounds may cause ridge discontinuities.
2. Excessively dry fingers lead to fragmented and low contrast ridges.
3. Sweat on fingerprints leads to smudge marks and connects parallel ridges.

While most algorithms are designed to operate on well defined ridge structures, the quality of fingerprint encountered during verification varies over a wide range as shown in Fig. 1. It is estimated that roughly 10% of the fingerprint encountered during verification can be classified as 'poor' [1]. The robustness of the fingerprint recognition system can be improved by incorporating an enhancement stage prior to feature extraction. Due to the non-stationary nature of the fingerprint image, general-purpose image processing algorithms are not very useful in this regard but only serve as a preprocessing step in the overall enhancement scheme. The majority the existing techniques are based on the use of contextual filters whose parameters depend on the properties of the local neighborhood. The filters themselves may be defined in spatial or in the Fourier domain.

---

\* Corresponding author: ssc5@eng.buffalo.edu



**Fig. 1. Fingerprint images of different quality. The quality decreases from left to right. (a) Good quality image with high contrast between the ridges and valleys (b) Insufficient distinction between ridges and valleys in the center of the image (c) Dry print**

---

### 1.1 Prior Related Work

O’Gorman et al. [2] proposed the use of contextual filters for fingerprint image enhancement for the first time. They used an anisotropic smoothing kernel whose major axis is oriented parallel to the ridges. For efficiency, they precompute the filter in 16 directions. The net result of the filter is that it increases contrast in a direction perpendicular to the ridges while performing smoothing in the direction of the ridges. Recently, Greenberg et al. [3] proposed the use of an anisotropic filter that is based on structure adaptive filtering [4]. Another approach based on directional filtering kernel was given by Hong et al. [5]. The algorithm uses a properly oriented Gabor kernel for performing the enhancement. Gabor filters have important properties from a signal processing perspective such as optimal joint space frequency resolution [6]. Gabor elementary functions form a very intuitive representation of fingerprint images since they capture the periodic, yet non-stationary nature of the fingerprint regions. This is by far, the most popular approach for fingerprint image enhancement.

Sherlock and Monro [7] perform contextual filtering completely in the Fourier Domain. Here, each image is convolved with precomputed filters of the same size as the image. The contextual filtering is actually accomplished by a ‘selector’ that uses the local orientation information to combine the results of the filter bank using appropriate weights for each output. The algorithm also accounts for the curvature of the ridges. In regions of high curvature, having a fixed angular bandwidth leads to processing artifacts and subsequently spurious minutiae.

### 1.2 Intrinsic Images

The *intrinsic images* represent the important properties of the fingerprint image as a pixel map. These include the ridge orientation image, the ridge frequency image and the region mask. The computation of the intrinsic images forms a very critical step in the feature extraction and in the matching process. Applications that require a reliable orientation image include enhancement [5, 7, 2, 8], singular point detection [9–11] and segmentation [12] and most importantly fingerprint classification [13–17]. The region mask is used to eliminate spurious fingerprint features [8, 5].

**Orientation Image** The orientation image  $\mathbf{O}$  represents the instantaneous ridge orientation at every point in the fingerprint image. There have been several approaches to estimate the orientation image of a fingerprint image. Here we discuss some popular approaches for computing the orientation image.

Except in the region of singularities such as core and delta, the ridge orientation varies very slowly across the image. Therefore, the orientation image is seldom computed at full-resolution. Instead each non-overlapping block of size  $W \times W$  of the image is assigned a single orientation that corresponds to the most probable or *dominant* orientation of the block. The horizontal and vertical gradients  $G_x(x, y)$  and  $G_y(x, y)$  respectively, are computed using simple gradient operators such as a Sobel mask [18]. The block orientation  $\theta$  is given by  $\theta = \frac{1}{2} \tan^{-1} \frac{G_{yy}}{G_{xx}}$ , where

$$G_{xy} = \sum_{u \in W} \sum_{v \in W} 2G_x(u, v)G_y(u, v) \quad (1)$$

$$G_{xx} = \sum_{u \in W} \sum_{v \in W} G_x^2(u, v) - G_y^2(u, v) \quad (2)$$

A rigorous derivation of the above relation is provided in [19]. The dominant orientation so obtained still contains inconsistencies caused by creases and ridge breaks. Utilizing the regularity property of the fingerprint, the orientation image is smoothed by vector averaging.

**Frequency Image** The ridge frequency is another intrinsic property of the fingerprint image. It is also a slowly varying property and hence is computed only once for each non-overlapping block of the image. It indicates the average inter-ridge distance within a block and is estimated based on the projection sum taken along a line oriented orthogonal to the ridges [5], or based on the variation of gray levels in a window oriented orthogonal to the ridge flow [20]. These methods depend upon the reliable extraction of the local ridge orientation. The projection sum forms a sinusoidal signal and the distance between any two peaks provides the inter-ridge distance. The frequency image so obtained may be further filtered to remove the outliers.

**Region Mask** The region mask indicates the parts of the image where ridge structures are present. It is also known as the foreground mask and is used to eliminate spurious features that may occur outside the fingerprint area.

## 2 Proposed Approach: STFT Analysis

We present a new fingerprint image enhancement algorithm based on contextual filtering in the Fourier domain. The fingerprint image may be thought of as a system of oriented texture with non-stationary properties. Therefore, traditional Fourier analysis is not adequate to analyze the image completely. We need to resolve the properties of the image both in space and also in frequency. We can extend the traditional one dimensional time-frequency analysis to two dimensional image signals to perform short

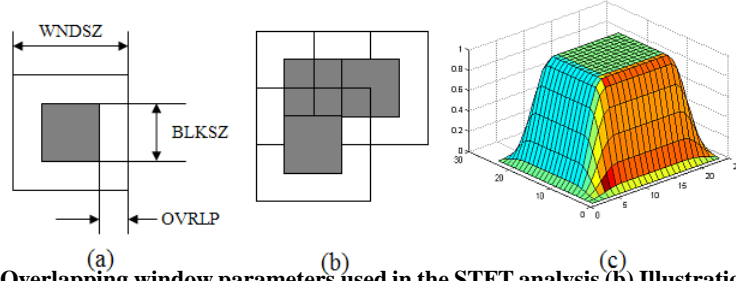


**Fig. 2. (a)Overlapping window parameters used in the STFT analysis (b) Illustration of how analysis windows are moved during analysis (b)Spectral window used in STFT analysis**

(time/space)-frequency analysis. In this section, we recapitulate some of the principles of 1D STFT analysis and show how it is extended to two dimensions for the sake of analyzing the fingerprint.

When analyzing a non-stationary 1D signal  $x(t)$  it is assumed that it is approximately stationary in the span of a temporal window  $w(t)$  with finite support. The STFT of  $x(t)$  of such a signal is represented by time frequency *atoms*  $X(\tau, \omega)$  [21] and is given by

$$X(\tau, \omega) = \int_{-\infty}^{\infty} x(t) \omega^*(t - \tau) e^{-j\omega t} dt \quad (3)$$

In the case of 2D signals such as a fingerprint image, the space-frequency *atoms* is given by

$$X(\tau_1, \tau_2, \omega_1, \omega_2) = \int_{-\infty}^{\infty} \int_{-\infty}^{\infty} I(x, y) W^*(x - \tau_1, y - \tau_2) e^{-j(\omega_1 x + \omega_2 y)} dx dy \quad (4)$$

Here  $\tau_1, \tau_2$  represent the spatial position of the two dimensional window  $W(x, y)$ .  $\omega_1, \omega_2$  represents the spatial frequency parameters. Figure 2 illustrates how the spectral window is parameterized. At each position of the window, it overlaps OVRLP pixels with the previous position. This preserves the ridge continuity and eliminates 'block' effects common with other block processing image operations. Each such analysis frame yields a single value of the dominant orientation and frequency in the region centered around  $(\tau_1, \tau_2)$ . However, unlike regular Fourier transform, the result of the STFT is dependent on the choice of the window  $w(t)$ . For the sake of analysis, any smooth spectral window such as hanning, hamming or even a gaussian [22] window may be utilized. However, since we are also interested in enhancing and reconstructing the fingerprint image directly from the Fourier domain, our choice of window is fairly restricted. We chose a  $12 \times 12$  window since it provides a good trade-off between local stationarity and processing complexity. Larger windows are unsuitable since the image will no longer be stationary within it. In order to provide suitable reconstruction during enhancement, we utilize a raised cosine window that tapers smoothly near the border and is unity at

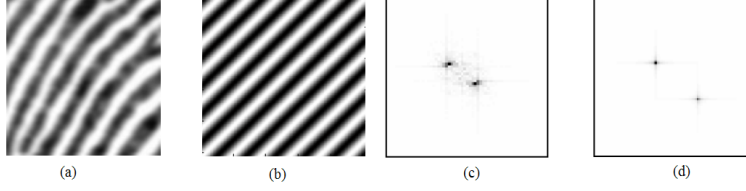


**Fig. 3. (a) Local region in a fingerprint image (b) Surface wave approximation (c,d) Fourier spectrum of the real fingerprint and the surface wave. The symmetric nature of the Fourier spectrum arrives from the properties of the Fourier transform for real signals [18]**

---

the center of the window. The raised cosine spectral window is obtained using

$$W(x, y) = \begin{cases} 1 & \text{if } (|x|, |y|) < \text{BLKSZ}/2 \\ \frac{1}{2} \left( 1 + \cos\left(\frac{\pi x}{\text{OVRLEP}}\right) \right) & \text{otherwise} \end{cases} \quad (x, y) \in [-W\text{NDSZ}/2, W\text{NDSZ}/2] \quad (5)$$

With the exception of the singularities such as core and delta any local region in the fingerprint image has a consistent orientation and frequency. Therefore, the local region can be modeled as a surface wave that is characterized completely by its orientation  $\theta$  and frequency  $f$  (See Fig. 3). It is these parameters that we hope to infer by performing STFT analysis. This approximation model does not account for the presence of local discontinuities but is useful enough for our purpose. A local region of the image can be modeled as a surface wave according to  $I(x, y) = A \{2\pi f \cos(x \cos(\theta) + y \sin(\theta))\}$

The parameters of the surface wave  $(f, \theta)$  may be easily obtained from its Fourier spectrum that consists of two impulses, whose distance from the origin indicates the frequency and angular location indicates the orientation of the wave. However, this straight forward approach is not very useful since the maximum response is prone to errors. Creases running across the fingerprint can easily put off such maximal response estimators. Instead, we propose a probabilistic approximation of the dominant ridge orientation and frequency. Representing the Fourier spectrum in polar form as  $F(r, \theta)$ , we can define a probability density function  $p(r, \theta)$  and the marginal density functions  $p(\theta)$ ,  $p(r)$  as

$$p(r, \theta) = \frac{|F(r, \theta)|^2}{\int_r \int_\theta |F(r, \theta)|^2} \quad (6)$$

$$p(r) = \int_\theta p(r, \theta) d\theta, p(\theta) = \int_r p(r, \theta) dr \quad (7)$$

## 2.1 Ridge Orientation Image

To compute the ridge orientation image, we assume that the orientation  $\theta$  is a random variable that has the probability density function  $p(\theta)$ . The expected value of the orientation may then be obtained by performing a vector averaging according to 8. The terms

$\sin(2\theta)$  and  $\cos(2\theta)$  are used to resolve the orientation ambiguity between orientations  $\pm 180^\circ$

$$E\{\theta\} = \frac{1}{2} \tan^{-1} \left\{ \frac{\int_{\theta} p(\theta) \sin(2\theta) d\theta}{\int_{\theta} p(\theta) \cos(2\theta) d\theta} \right\} \quad (8)$$

However, if there is a crease in the fingerprints that spans several analysis frames, the orientation estimation will still be wrong. The estimate will also be inaccurate when the frame consists entirely of unrecoverable regions with poor ridge structure or poor ridge contrast. In such instances, we can estimate the ridge orientation by considering the orientation of its immediate neighborhood. The resulting orientation image  $O(x,y)$  is further smoothened using vectorial averaging. The smoothened image  $O'(x,y)$  is obtained using

$$O'(x,y) = \frac{1}{2} \left\{ \tan^{-1} \frac{\sin(2O(x,y)) * W(x,y)}{\cos(2O(x,y)) * W(x,y)} \right\} \quad (9)$$

. Here  $W(x,y)$  represent a gaussian smoothening kernel. It has been our experience that a smoothening kernel of size 3x3 applied repeatedly provides a better smoothening result than using a larger kernel of size 5x5 or 7x7.

## 2.2 Ridge Frequency Image

The average ridge frequency is estimated in a manner similar to the ridge orientation. We can assume the ridge frequency to be a random variable with the probability density function  $p(r)$  as in Eq 7. The expected value of the ridge frequency is given by  $E\{r\} = \int_r p(r)rdr$

The frequency map so obtained is smoothened by process of isotropic diffusion. Simple smoothening cannot be applied since the ridge frequency is not defined in the background regions. The smoothened is obtained by the following.

$$F'(x,y) = \frac{\sum_{u=x-1}^{x+1} \sum_{v=y-1}^{y+1} F(u,v)W(u,v)I(u,v)}{\sum_{v=y-1}^{y+1} W(u,v)I(u,v)} \quad (10)$$

This is similar to the approach proposed in [5]. Here  $H,W$  represent the height and width of the frequency image.  $W(x,y)$  represents a gaussian smoothening kernel of size 3x3. The indicator variable  $I(x,y)$  ensures that only valid ridge frequencies are considered during the smoothening process.  $I(x,y)$  is non zero only if the ridge frequency is within the valid range (3-25 pixels per ridge [5]).

## 2.3 Region Mask

The fingerprint image may be easily segmented based on the observation that the surface wave model does not hold in regions where ridges do not exist. In the areas of background and noisy regions, there is very little energy content in the Fourier spectrum. We define an energy image  $E(x,y)$ , where each value indicates the energy content of the corresponding block. The fingerprint region may be differentiated from the background by thresholding the energy image. We take the logarithm values of the energy

to compress the large dynamic range to a linear scale.

$$E(x, y) = \log \left\{ \int_r \int_\theta |F(r, \theta)|^2 \right\} \quad (11)$$

The resulting binary image is processed further to retain the largest connected component and binary morphological processing [23].

**Coherence Image** Enhancement is especially problematic in regions of high curvature close to the core and deltas that have more than one dominant direction. Excessively narrow angular bandwidth causes spurious artifacts and ridge discontinuities in the reconstructed image. Sherlock and Monro [7] used a piece wise linear dependence between the angular bandwidth of their filter and the ridge curvature. However, this requires a reasonable estimation of the singular point location. Most algorithms for singular point location [9, 10] are not reliable in noisy and poor quality images. Therefore we rely on a flow-orientation/angular coherence measure [24] that is more robust than singular point detection. The coherence is related to dispersion measure of circular data and is given by

$$C(x_0, y_0) = \frac{\sum_{(i,j) \in W} |\cos(\theta(x_0, y_0) - \theta(x_i, y_i))|}{W \times W} \quad (12)$$

The coherence is high when the orientation of the central block  $\theta(x_0, y_0)$  is similar to each of its neighbors  $\theta(x_i, y_i)$ . In a fingerprint image, the coherence is expected to be low closer to regions of high curvature. We therefore utilize this coherence measure to adapt the angular bandwidth of the directional filter.

## 2.4 Enhancement

The algorithm consists of two stages. The first stage consists of STFT analysis outlined before and is responsible for computing all the intrinsic images of the fingerprint. The image is divided into overlapping windows as shown in Fig. 2. It is assumed that the image is stationary within this small window and can be modeled approximately as a surface wave. The fourier spectrum of this small region is analyzed and probabilistic estimates of the ridge frequency and ridge orientation are obtained as outlined before. In each window we apply a filter that is tuned to the radial frequency and aligned with the dominant ridge direction. The filter itself is separable in angle and frequency and is identical to the filters mentioned in [7] and is given by

$$H(\rho, \phi) = H_\rho(\rho)H_\phi(\phi) \quad (13)$$

$$H_\rho(\rho) = \sqrt{\left[ \frac{(\rho\rho_{BW})^{2n}}{(\rho\rho_{BW})^{2n} + (\rho^2 - \rho_0^2)^{2n}} \right]} \quad (14)$$

$$H_\phi(\phi) = \begin{cases} \cos^2 \frac{\pi}{2} \frac{(\phi - \phi_c)}{\phi_{BW}} & \text{if } |\phi| < \phi_{BW} \\ 0 & \text{otherwise} \end{cases} \quad (15)$$



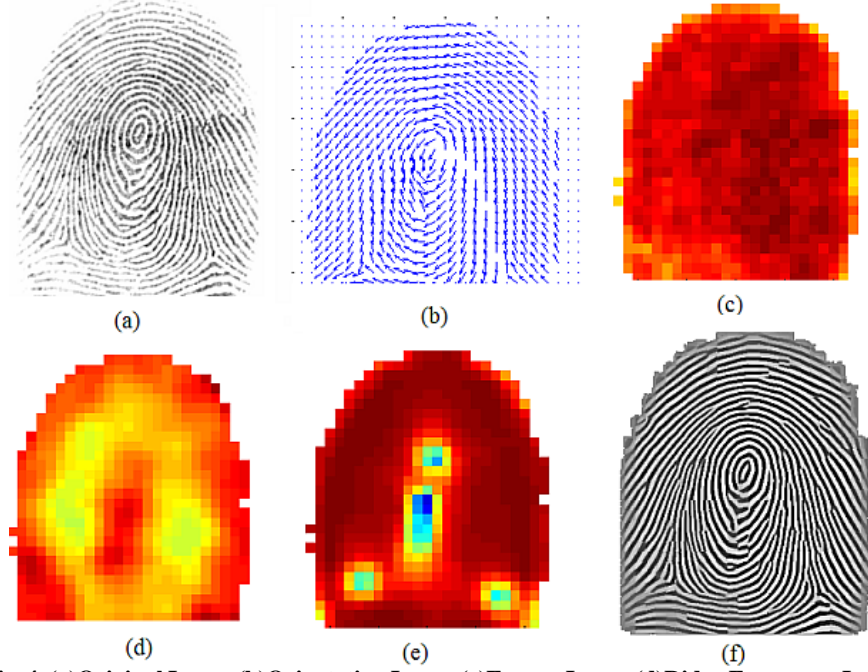


**Fig. 4. (a)Original Image (b)Orientation Image (c)Energy Image (d)Ridge Frequency Image (e)Angular Coherence Image (f)Enhanced Image**

---

Here  $H_\rho(\rho)$  is a band-pass butterworth filter with center defined by  $\rho_0$  and bandwidth  $\rho_{BW}$ .  $\rho_0$  is derived from the intrinsic orientation image while the bandwidth  $\rho_{BW}$  is chosen to be inversely proportional to the angular coherence measure. The angular filter is a raised cosine filter in the angular domain with support  $\phi_{BW}$  and center  $\phi_c$ . The enhanced image is reconstructed by tiling the results of enhancement of each local window. Figure 5 shows the results of enhancement on some sample images.

### 3 Experimental Evaluation

While the effect of the enhancement algorithm may be gauged visually, the final objective of the enhancement process is to increase the accuracy of the recognition system. We evaluated the effect of our enhancement on a set of 800 images (100 users, 8 images each) derived from FVC2002 [25] DB3 database. In order to obtain the performance characteristics such as EER (Equal Error Rate) we perform a total of 2800 genuine (each instance of a finger is compared with the rest of the instances resulting in  $(8 \times 7)/2$  tests per finger) comparison and 4950 impostor comparisons (the first instance of each finger is compared against the first instance of all other fingers resulting in a total of  $(100 \times 99)/2$  tests for the entire database). We used NIST's NFIS2 open source software

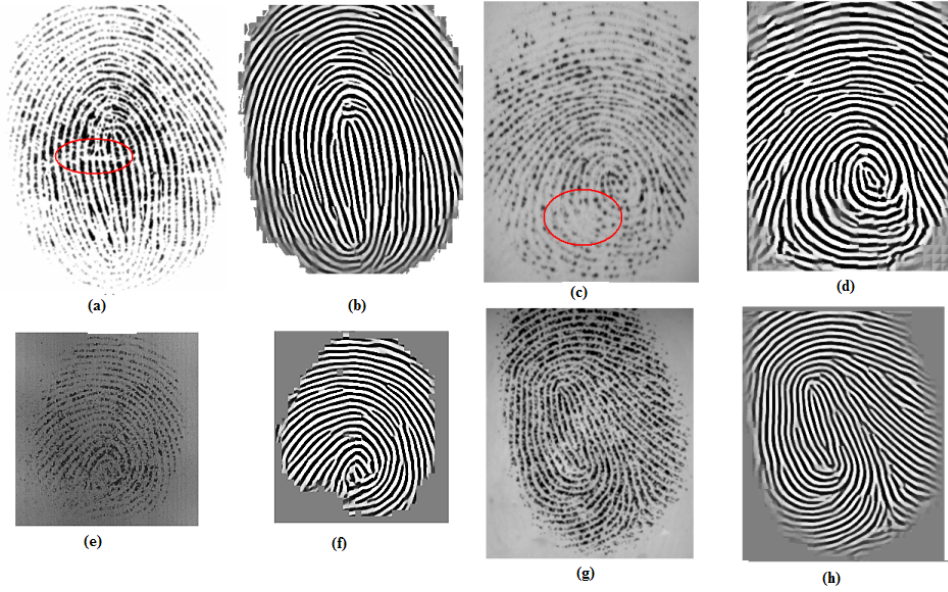


**Fig. 5. Original and enhanced images (Samples from FVC2002 [25] database): (a,b)DB1 database,(c,d)DB2 (e,f) DB3, (g,h) DB4**

(<http://fingerprint.nist.gov>) for feature extraction and matching. The summary of the results is provided in Table 1.

## 4 Summary

The performance of a fingerprint feature extraction and matching algorithms depend critically upon the quality of the input fingerprint image. We presented a new fingerprint image enhancement algorithm based on STFT analysis and contextual/non-stationary filtering in the Fourier domain to address this problem. The proposed approach obviates the need for multiple algorithms to compute the intrinsic images and replaces it with a single unified approach. The algorithm utilized complete contextual information including instantaneous frequency, orientation and even orientation coherence/reliability. We performed an objective evaluation of the enhancement algorithm by considering the

**Table 1. Effect on enhancement on the final recognition accuracy**

DB3 Results	Equal Error Rate
Without Enhancement	10.35%
With Enhancement	8.5%
Improvement	17%

improvement in matching accuracy for poor quality fingerprints and showed that it results in net improvement in recognition rate. (The matlab code for the enhancement is available for download at <http://www.cubs.buffalo.edu>).

## References

1. Maio, D., Maltoni, D., Jain, A.K., Prabhakar, S.: Handbook of Fingerprint Recognition. Springer Verlag (2003)
2. O’Gormann, L., J.V.Nickerson: An approach to fingerprint filter design. *Pattern Recognition* **22** (1989) 29–38
3. S., G., M., A., D., K., I., D.: Fingerprint image enhancement using filtering techniques. In: International Conference on Pattern Recognition. Volume 3. (2000) 326–329
4. Yang, G.Z., Burger, P., Firmin, D.N., Underwood, S.R.: Structure adaptive anisotropic image filtering. *Image and Vision Computing* **14** (1996) 135–145
5. Hong, L., Wang, Y., Jain, A.K.: Fingerprint image enhancement: Algorithm and performance evaluation. *Transactions on PAMI* **21** (1998) 777–789
6. Qian, S., Chen, D.: Joint Time-Frequency Analysis, Methods and Applications. Prentice Hall (1996)
7. B.G.Sherlock, D.M.Monro, K.Millard: Fingerprint enhancement by directional fourier filtering. In: Visual Image Signal Processing. Volume 141. (1994) 87–94
8. Connell, J., Ratha, N.K., Bolle, R.M.: Fingerprint image enhancement using weak models. In: IEEE International Conference on Image Processing. (2002)
9. Srinivasan, V.S., Murthy, N.N.: Detection of singular points in fingerprint images. *Pattern Recognition* **25** (1992) 139–153
10. Bazen, A.M., Gerez, S.: Extraction of singular points from directional fields of fingerprints. (2001)
11. Kawagoe, Tojo: Fingerprint pattern classification. *Pattern Recognition* **17** (1987) 295–303
12. Mehre, B.M., Murthy, N.N., Kapoor, S., Chatterjee, B.: Segmentation of fingerprint images using the directional image. *Pattern Recognition* **20** (1987) 429–425
13. Cappelli, R., Lumini, A., Maio, D., Maltoni, D.: Fingerprint classification by directional image partitioning. *IEEE Transactions on Pattern Analysis and Machine Intelligence* **21** (1999)
14. Candela, G.T., Grother, P.J., Watson, C.I., Wilkinson, R.A., Wilson, C.L.: Pcasys - a pattern-level classification automation system for fingerprints (1995)
15. Karu, K., Jain, A.: Fingerprint classification (1996)
16. Rao, K., Balck, K.: Type classification of fingerprints: A syntactic approach. *IEEE Transactions on Pattern Analysis and Machine Intelligence* **2** (1980) 223–231
17. Jain, A.K., Prabhakar, S., Hong, L.: A multichannel approach to fingerprint classification. *IEEE Transactions on Pattern Analysis and Machine Intelligence* **21** (1999) 348–359
18. Gonzalez, Woods, Eddins: Digital Image Processing. Prentice Hall (2004)
19. Kaas, M., Witkin, A.: Analyzing oriented patterns. *Computer Vision Graphics Image Processing* **37** (1987) 362–385
20. D., M., D., M.: Neural network based minutiae filtering in fingerprint images. In: 14th International Conference on Pattern Recognition. (1998) 1654–1658
21. Haykin, S., Veen, B.V.: Signals and Systems. John Wiley and Sons (1999)
22. Rabiner, Schafer: Digital Processing of Speech Signals. Prentice Hall International (1978)
23. Sonka, Hlavac, Boyle: Image Processing, Analysis and Machine Vision, second edition. Thomson Asia (2004)
24. Rao, A.R.: A Taxonomy of Texture Descriptions. (Springer Verlag)
25. : (Fingerprint verification competition) <http://bias.csr.unibo.it/fvc2002/>.